Longitudinal spin fluctuations in nickel

P. Böni
Paul Scherrer Institut, CH-5232 Villigen PSI, Switzerland

J. L. Martínez
Institut Laue Langevin, F-38042 Grenoble CEDEX, France

J. M. Tranquada
Brookhaven National Laboratory, Upton, New York 11973-5000
(Received 22 May 1990; revised manuscript received 20 August 1990)

The longitudinal, transverse, and paramagnetic spin fluctuations in Ni have been measured near T_C by means of polarized neutron scattering in the momentum range $0.06 < q < 0.18$ Å^{-1}. In transverse scans, spin-wave peaks at $\omega_q = Dq^2$ appear as expected from previous measurements performed with unpolarized neutrons. The longitudinal fluctuations are quasielastic, in agreement with predictions of a recent mode-mode coupling theory and renormalization-group theory. The data indicate that the longitudinal dynamical scaling function is smaller than 1 just below T_C. The scaling function for the paramagnetic scattering is shown to be in agreement with the Résibois-Piette scaling function for energy scales up to $k_B T_C$. The measured field dependence of the scattering is rather weak, indicating that the internal fields H are rather large. Therefore it was impossible to observe the $H^{-1/2}$ divergence of $\chi_L(q \to 0)$ that is predicted for the isotropic Heisenberg model in three dimensions. In contrast, we found $\chi_L(q \to 0) \propto (1 - T/T_C)^{-\gamma}$, which also appears to be a result of the internal fields. The q dependence of χ_L is Lorentzian-like. The T dependence of the correlation length indicates critical behavior. These features closely resemble the behavior of the paramagnetic fluctuations, and they are in agreement with results obtained with use of expansion techniques.

I. INTRODUCTION

Despite a great deal of theoretical and experimental activity concerning the spin dynamics of isotropic ferromagnets, many properties are still not well understood. For example, the interplay between localized and itinerant magnetism on the one hand and the properties of the longitudinal fluctuations on the other hand are still unresolved topics. Another intriguing subject, namely, the influence of the dipolar interactions on the critical dynamics above the Curie temperature T_C, is now better understood thanks to the pioneering work by Frey, Schwabl, and Thoma[1,2] (see also Aberger and Folk[3]). Some of the theoretical results have been verified in recent experiments. The influence of the dipolar interactions on the spin dynamics below T_C, however, has not yet been worked out in detail.

The field and temperature dependences of the longitudinal fluctuations have been investigated both theoretically and experimentally for many years. In 1940, Holstein and Primakoff[4] showed, by means of the spin-wave theory, that the longitudinal susceptibility $\chi_L(q=0)$ of an isotropic ferromagnet diverges at all temperatures below T_C as $1/\sqrt{H}$, a result that has since been verified theoretically many times, in particular, by means of renormalization-group methods. The divergence of χ_L is induced by the divergence of the transverse modes, which, in turn, is caused by the fact that, due to the rotational invariance of the Heisenberg Hamiltonian in three dimensions, there is a spontaneous symmetry breaking that does not involve any energy (Goldstone theorem), i.e., the spin-wave spectrum has no gap. The occurrence of these singularities prompted detailed investigations of the equation of state and of the correlation functions by means of the renormalization-group theory[5–10] and mode-mode coupling calculations.[1,11,12] The results are still awaiting an experimental verification.

Unfortunately, the divergence of χ_L at temperatures below T_C has not yet been detected unambiguously. A scaling analysis of magnetization measurements in EuS yielded a first indication of a $H^{-1/2}$ divergence of χ_L.[13] The search for such a singularity by means of neutron scattering in EuO (Ref. 14) and Pd-10 at. % Fe (Ref. 15) has so far been unsuccessful.

The theoretical picture for the frequency dependence of the longitudinal susceptibility $\chi_L(q,\omega)$ is less well resolved. The predicted spectral features range from quasielastic peaks[1,9] to spin-wave-like excitations[11,12,16] or a mixture of both. Unpolarized neutron-scattering experiments on Fe,[17] Ni,[18] and EuO (Ref. 14) seemed to support the conjecture that $\chi_L(q,\omega)$ has an inelastic shape because no quasielastic peak at $E=0$ was discernible, in contrast to antiferromagnets such as $RbMnF_3$, where a quasielastic component was clearly observed near T_N.[19]

Recently Mitchell, Cowley, and Pynn[15] have used polarized neutron scattering and demonstrated that $\chi_L(q,\omega)$ is purely quasielastic in Pd–10 at. % Fe. It became apparent that the linewidth Γ of the longitudinal

component is comparable with the spin-wave energy (peak position of the transverse fluctuations). This explains why the frequency dependence of $\chi_L(q,\omega)$ was not observed in previous experiments with unpolarized neutrons. Unfortunately, the data are not precise enough to test most of the theoretical predictions. Astonishingly, Γ seems to depend rather weakly on q.

We believe that Pd–10 at. % Fe is not an ideal system for the investigation of χ_L because of (i) the large incoherent cross section, (ii) the possibility of impurity scattering of the electrons in alloys[20] such as Pd–10 at. % Fe and Invar $Fe_{65}Ni_{35}$,[21] and the reentrant spin glass $Fe_{28}Cr_{72}$,[22] which could distort the dynamics of the longitudinal fluctuations near T_C, and (iii) the creation of strain fields or anisotropy fields in the crystal that may quench the $1/\sqrt{H}$ singularity in $\chi_L(0)$.

In order to circumvent the above difficulties, we decided to investigate the longitudinal susceptibility in an isotopically pure single-crystal ^{60}Ni by means of polarized neutron scattering. The following reasons have guided us to use this ferromagnet: (i) ^{60}Ni is a single element, monoisotopic ferromagnet, and therefore, the incoherent scattering is small. (ii) The magnetic scattering of Ni near T_C is similar to the scattering from a localized ferromagnet and is well known.[23–26] According to Hertz,[27] there is no way to distinguish an itinerant from a localized-spin magnet by studying its critical fluctuations. (iii) The dipolar interactions are weak compared with other well-known ferromagnets such as EuO and EuS, i.e., $q_D \simeq 0.013$ Å^{-1} (Ref. 28), so that it is possible to observe χ_L without interference of dipolar interactions. (iv) T_C is reasonably low, and hence a simple and small furnace can be used.

We should emphasize that this study is a first attempt to characterize the longitudinal fluctuations in Ni. We believe that it is important to measure the spin dynamics first and then the statics in order to sort out nuclear and background scattering that may remain unobserved in a measurement of $S(q)=\int S(q,\omega)d\omega$.

II. EXPERIMENT

The neutron-scattering experiments were conducted on the polarized triple-axis spectrometer IN20 at the High Flux Reactor at the Institut Laue Langevin. Heusler crystals set for the (111) reflection were used as monochromator and analyzer. The final neutron energy E_F was kept fixed at 14.7 meV, and the collimations were all 40′. Higher-order neutrons were removed by means of a pyrolytic graphite filter that was placed after the sample.

The large (25 g) isotopically enriched single-crystal ^{60}Ni was mounted with the [111] axis horizontal inside a specially designed evacuated furnace that fitted in between the pole pieces of an electromagnet. Because of the depolarization of the neutron beam by the orientational averaging of the magnetic domains, we conducted most measurements in a vertical field of 1.1 kOe near the (111) Bragg reflection. This value was large enough to ensure a reasonable polarization of the beam, but yet sufficiently small that the longitudinal fluctuations were not quenched. The Curie temperature $T_C=631\pm0.5$ K was determined by measuring the flipping ratio of the (111) Bragg reflection in a field of 2 Oe. The temperature control was stable to within ±0.3 K over the period of our measurements. The lattice constant of Ni is 3.53 Å, and the reciprocal lattice spacing corresponding to the (111) reflection is 3.07 Å^{-1}.

Before going into further details of our experiment, we explain first the procedure for measuring the longitudinal fluctuations in an isotropic ferromagnet. The general expression for the differential magnetic cross section for neutrons is[29]

$$\frac{d^2\sigma}{d\Omega\, d\omega}=\gamma_0^2\frac{k_f}{k_i}|\tfrac{1}{2}gF(\mathbf{Q})|^2e^{-2W}\sum_{\alpha,\beta}(\delta_{\alpha\beta}-\hat{Q}_\alpha\hat{Q}_\beta)\times S^{\alpha\beta}(\mathbf{Q},\omega)\ , \tag{1}$$

where $\gamma_0^2=0.291$ barn/sr, k_f and k_i are the wave vectors of the final and incident neutrons, g is the gyromagnetic ratio, $F(\mathbf{Q})$ is the form factor, and $\exp(-2W)$ is the Debye-Waller factor. $S^{\alpha\beta}$ is the spatial and temporal Fourier transform of the spin-spin correlation function for the Cartesian components α and β. The term $\delta_{\alpha\beta}-\hat{Q}_\alpha\hat{Q}_\beta$ selects those components of the scattering law that are perpendicular to the scattering vector $\mathbf{Q}$. In the isotropic case, $\alpha=\beta$. This selection rule allows one to measure the longitudinal component even with unpolarized neutrons. For instance, if a ferromagnetic sample is saturated in a magnetic field $\mathbf{H}\|\mathbf{Q}$, then unpolarized neutrons are only scattered by transverse fluctuations. In zero field, the scattering contains longitudinal fluctuations as well. By subtracting the properly weighted spectra from each other one can extract $\chi_L(q,\omega)$. We have used this procedure in preliminary measurements on ^{64}Ni in order to obtain a qualitative picture of $\chi_L(q,\omega)$.[30]

For polarized neutrons, we have an additional selection rule, namely, if the spin fluctuations are parallel to the polarization $\mathbf{P}$ of the neutrons (longitudinal), the scattering is non-spin-flip, and if the spin fluctuations are perpendicular (transverse) to $\mathbf{P}$, the scattering is spin-flip. Table I gives a summary of these rules. Obviously, the longitudinal fluctuations cannot be measured with a field parallel to $\mathbf{Q}$.

From inspection of Table I we see that the neutron-scattering cross section also contains nonmagnetic contributions that have to be removed before the data can e compared with a particular cross section. The following procedure for the extraction of the magnetic scattering

TABLE I. Magnetic σ_M^T, σ_M^L, nuclear σ_N, nuclear-spin-incoherent cross sections $\sigma_{\rm NSI}$ for the polarization setup; bg=background. $I_\Delta=I_{\rm VF}^{+\,+}-I_{\rm VF}^{+\,-}=\sigma_N-\frac{1}{3}\sigma_{\rm NSI}$ for $T>T_C$, since $\sigma_M^L=\sigma_M^T$ for the q range under investigation. $\sigma_{\rm NSI}\simeq0$ for the present experiment.

	Flipper on (+/−)	Flipper off (+/+)
Vertical field (VF)⊥Q	$\frac{1}{2}\sigma_M^T+\frac{2}{3}\sigma_{\rm NSI}+$bg	$\sigma_N+\frac{1}{2}\sigma_M^L+\frac{1}{3}\sigma_{\rm NSI}+$bg

was adopted.

(i) Measure the transverse and the longitudinal spin fluctuations at several temperatures below T_C as well as at one temperature above T_C.

(ii) Correct the raw data for the finite flipping ratio R of the neutron beam ($R=3.6$ at $0.97T_C$, 4.6 at $0.98T_C$, 5.9 at $0.99T_C$, and 11.1 at $1.01T_C$):

$$I_L(T)=\frac{R}{R-1}I_{\text{off}}(T)-\frac{1}{R-1}I_{\text{on}}(T)\ ,$$

$$I_T(T)=\frac{R}{R-1}I_{\text{on}}(T)-\frac{1}{R-1}I_{\text{off}}(T)\ ,$$

where I_{off} Is the non-spin-flip scattering and I_{on} is the spin-flip scattering.

(iii) Separate out the phonons from the corrected scans above T_C by taking the difference (see Table I)

$$I_\Delta=I_L(1.013T_C)-I_T(1.013T_C)\ .$$

(iv) Subtract I_Δ from the corrected longitudinal scans $I_L(T<T_C)$.

(v) Correct for the energy dependence of the counting time caused by higher-order neutrons in the incident neutron beam.[31]

During the course of the data analysis, it became apparent that the contribution of the spin-incoherent scattering was not visible and could safely be neglected. We confirmed that the flipping ratio was independent of energy by comparing phonon intensities measured in the spin-flip and non-spin-flip scattering configuration.

III. RESULTS

In Figs. 1 and 2 we present some typical raw data that have been measured below T_C in order to discuss qualitatively (see Table I) the spectral shape of the magnetic scattering and the corrections that we applied to the data. The measurements were conduced at $0.97T_C$ in an applied field of 1.1 kOe.

In the transverse scan (flipper on) at (1.03 1.03 1.03) ($q=0.092$ Å^{-1}), we clearly observe two spin-wave peaks at ± 1 meV. The spectrum closely resembles unpolarized beam measurements.[18] At larger q, i.e., at (1.05 1.05 1.05), the spin-wave peaks occur near 3 meV. In addition, we observe a weak phonon peak at 6 meV, which appears because of the finite polarization of the neutron beam. The resolution limited peak around $E=0$ is due to scattering from the sample and its environment, which is also visible in the flipper-on channel because of the finite flipping ratio. The longitudinal scan at (1.03 1.03 1.03) is dominated by a broad quasielastic peak and a phonon peak near 3.5 meV. The longitudinal scattering at (1.05 1.05 1.05) is rather involved. After inspection of Table I and a comparison with unpolarized beam data, it is apparent that the elastic peak is composed of spin-incoherent scattering and elastic scattering from sample and sample container. The peak at 3.5 meV is composed of a transverse phonon that is still visible, although the vertical resolution was good (60 min), and that part of the

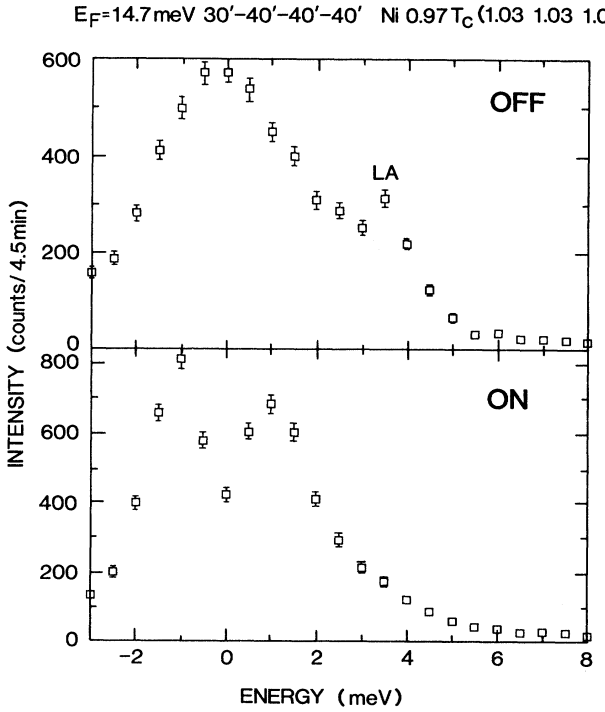

FIG. 1. Longitudinal (flipper off) and transverse scattering (flipper on) at (1.03, 1.03, 1.03) for $T=0.97T_C$ and $H=1.1$ kOe. No corrections have been applied to the data. LA is the longitudinal-acoustic phonon.

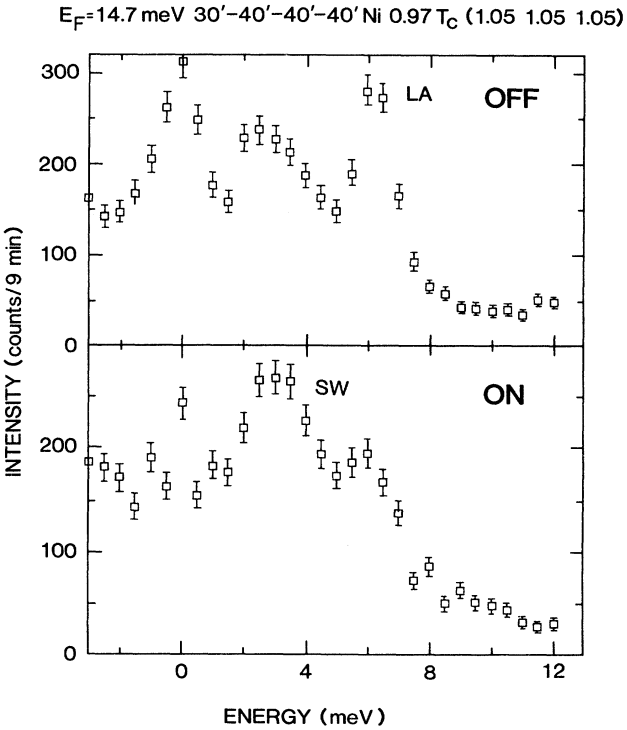

FIG. 2. Same as Fig. 1 for (1.05 1.05 1.05).

spin-wave scattering that appears from the flipper-on channel because of the finite flipping ratio. The narrow peak at 6.2 meV is the longitudinal acoustic phonon. These peaks are sitting on top of the broad magnetic scattering whose spectral shape is quite different from the shape of the transverse scattering. The transverse and longitudinal intensities are comparable.

In Fig. 3, we show scans at (1.06 1.06 1.06) after correcting for the finite flipping ratio. The profiles of the magnetic scattering are now clearly visible, namely, a quasielastic response for the longitudinal cross section and spin waves in the transverse cross section. Note that this scan corresponds to the largest q where we performed our measurmeents. The longitudinal scattering looks very similar as unpolarized neutron scattering from paramagnetic fluctuations.[23,24] From a comparison of the scattering around $E=0$ meV, we learn that the nuclear-spin-incoherent (NSI) cross section σ_{NSI} is very small since there is no elastic peak in the transverse scan. Therefore, the elastic peak in the longitudinal scan is nonmagnetic scattering from the sample and the furnace. It can be removed, together with the phonon scattering by subtraction of I_{Δ} (see also Table I). Figure 4 shows a typical example of a difference scan above T_C.

The data presented in the following figures incorporate all of the corrections mentioned above. We have corrected the data for the effect of higher-order neutrons on the

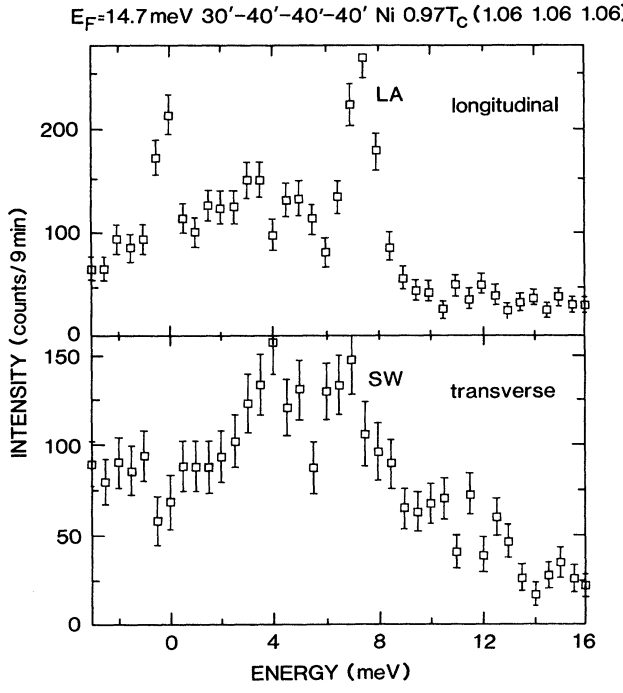

FIG. 3. Scans at (1.06 1.06 1.06) and $T=0.97T_C$ after correcting for the finite flipping ratio $R=3.64$. The profile of the magnetic scattering is rather different for the flipper-on and -off channels. The elastic scattering is obviously nonmagnetic. The absence of an elastic peak in the transverse scan indicates that the spin-incoherent scattering can be neglected.

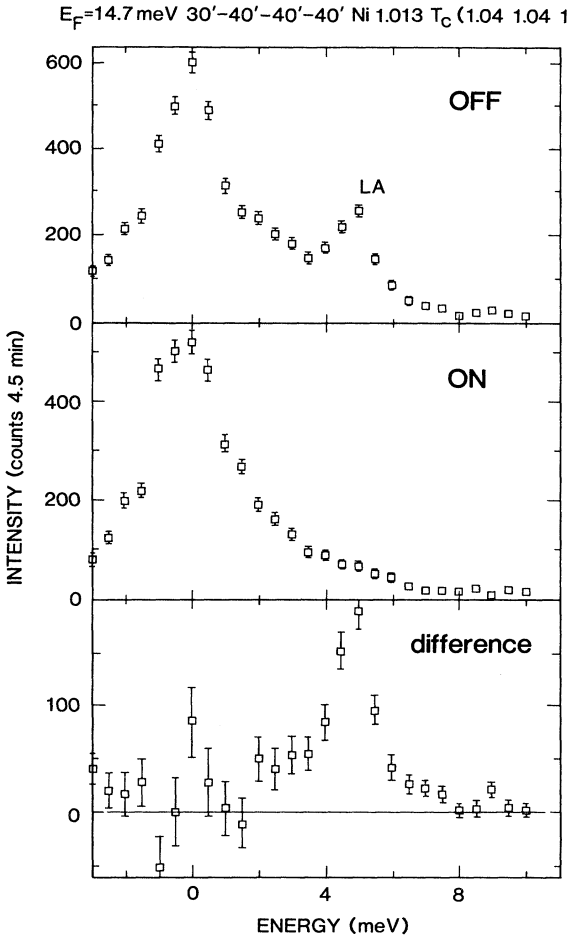

FIG. 4. Determination of the nuclear scattering from scans at (1.04 1.04 1.04) and $T=1.013T_C$. The difference scans contain the nuclear-scattering contributions in the non-spin-flip scattering cross section.

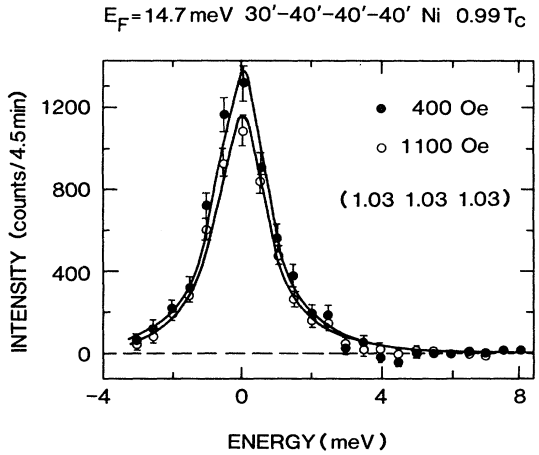

FIG. 5. Field dependence of the longitudinal scattering at $T=0.987T_C$. The intensity decreases only slightly with increasing field. The solid lines are Lorentzian fits to the data.

counting time as discussed above,[32] and we have subtracted an energy-independent background of 1 count/min. The counting time at the largest q did not exceed 15 min.

The field dependence of the longitudinal scattering at (1.03 1.03 1.03) is shown in Fig. 5. The intensity decreases slightly with increasing field, indicating that the scattering from the sample is not significantly distorted by the applied external field. We point out that the longitudinal susceptibility is expected to diverge only at $q=0$ as $H^{-1/2}$.

The q dependence of the longitudinal fluctuations is shown in Fig. 6. The peak intensity rapidly decreases and the linewidth increases with increasing q. There is no indication of any peaks at finite energy, although the spin waves are still very well defined (not shown) at the corresponding q's in the spin-flip scattering cross section. The general behavior of $\chi_L(q,\omega)$ closely resembles the paramagnetic scattering reported in previous studies.

In order to put our results on a more quantitative basis, we analyzed all the data in terms of the scattering function

$$S^{\alpha\alpha}(\mathbf{Q},\omega)=\frac{\chi_\alpha(\mathbf{Q})}{\chi_0}F_\alpha(\mathbf{Q},\omega)\frac{\omega/k_BT}{1-\exp(-\omega/k_BT)}\ , \tag{2}$$

where χ_0 is the susceptibility for a system of noninteracting spins, $\hbar=1$, and the spectral weight function is normalized:

$$\int_{-\infty}^{\infty}F_\alpha(\mathbf{Q},\omega)d\omega=1\ . \tag{3}$$

For the wave-vector-dependent susceptibility χ_α, $\alpha=L$ (longitudinal), T (transverse), or P (paramagnetic), we assume, in analogy to mean-field theory[29] and previous neutron scattering work on EuO,[14]

$$\chi_i(q)=\chi_i(0)\frac{\kappa_i^2}{\kappa_i^2+q^2}\ , \tag{4}$$

where κ_i are correlation lengths, and $\chi_i(0)$ are bulk susceptibilities. As a shape function for the magnetic scattering, we assume Lorentzians centered at the spin-

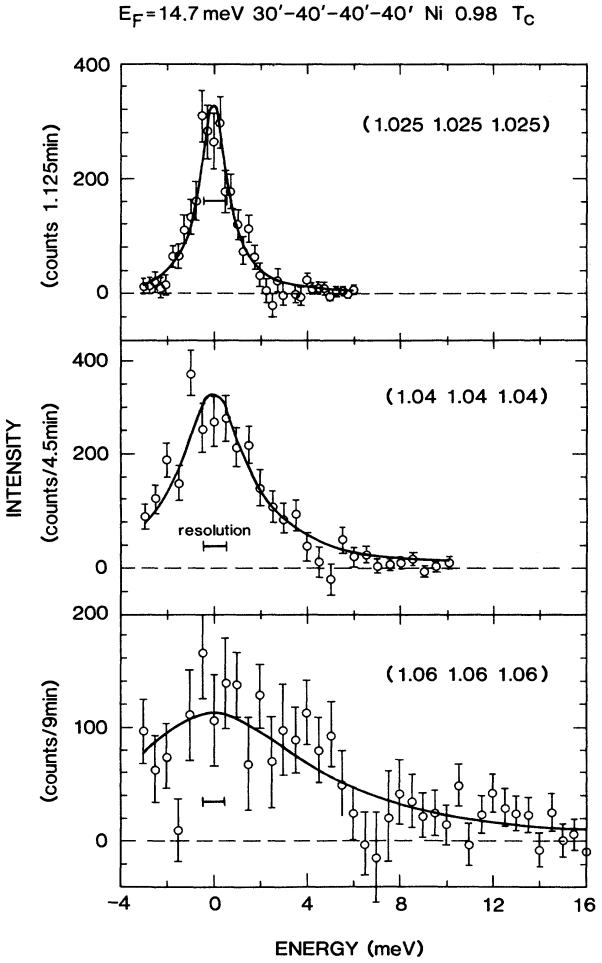

FIG. 6. q dependence of the longitudinal scattering at $0.98T_C$. The spectrometer resolution is indicated by a horizontal bar. The solid lines are fits to the data.

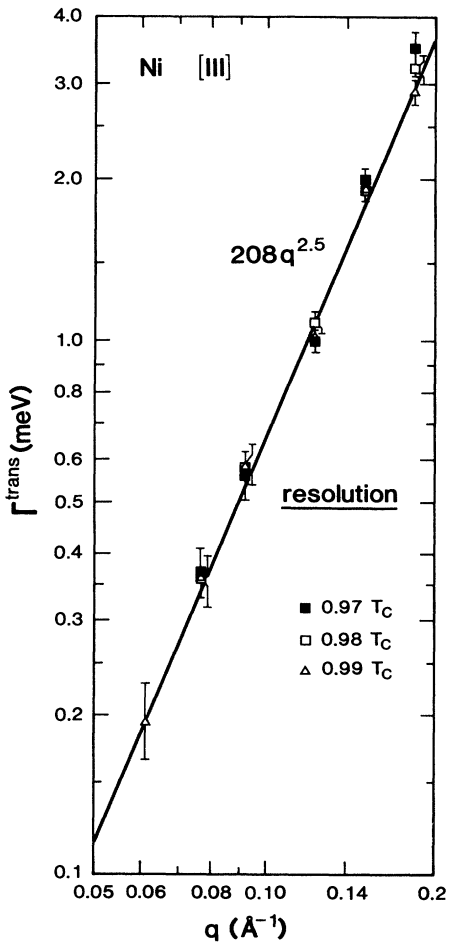

FIG. 7. The linewidth of the spin waves is roughly proportional to $q^{2.5}$. Γ is almost independent of T.

wave-energy $\omega_q = Dq^2$:

$$F(\mathbf{Q},\omega) = \frac{1}{2\pi}\left[\frac{\Gamma}{(\omega-\omega_q)^2+\Gamma^2} + \frac{\Gamma}{(\omega+\omega_q)^2+\Gamma^2}\right], \quad (5)$$

where D is the stiffness. The linewidth is parametrized by $\Gamma = A^{\text{eff}} q^{2.5}$. For the analysis of the quasielastic scattering, we fixed the stiffness at $D=0$. The magnetic cross section is convolved with the resolution function in four dimensions, and for each q the parameters D and A^{eff} were determined by using a nonlinear least-squares fitting routine. The parametrizations ensure that the dispersion of the magnetic scattering is properly taken into account during the convolution. The solid lines in Figs. 5 and 6 indicate such fits. Finally, the linewidths (Figs. 7 and 8) and the spin-wave energies (Fig. 9) were calculated for each q from the fitted values of D and A^{eff}.

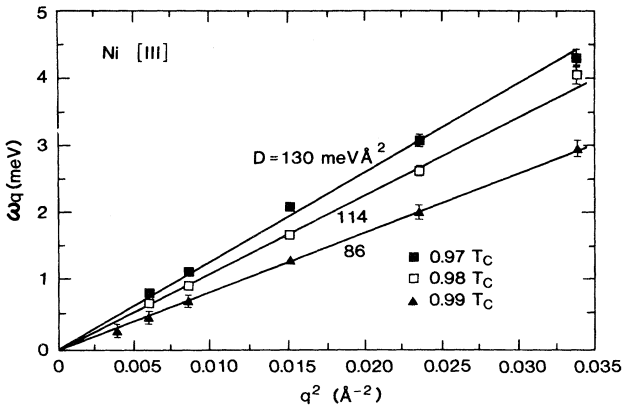

FIG. 9. q and T dependence of the spin-wave excitations.

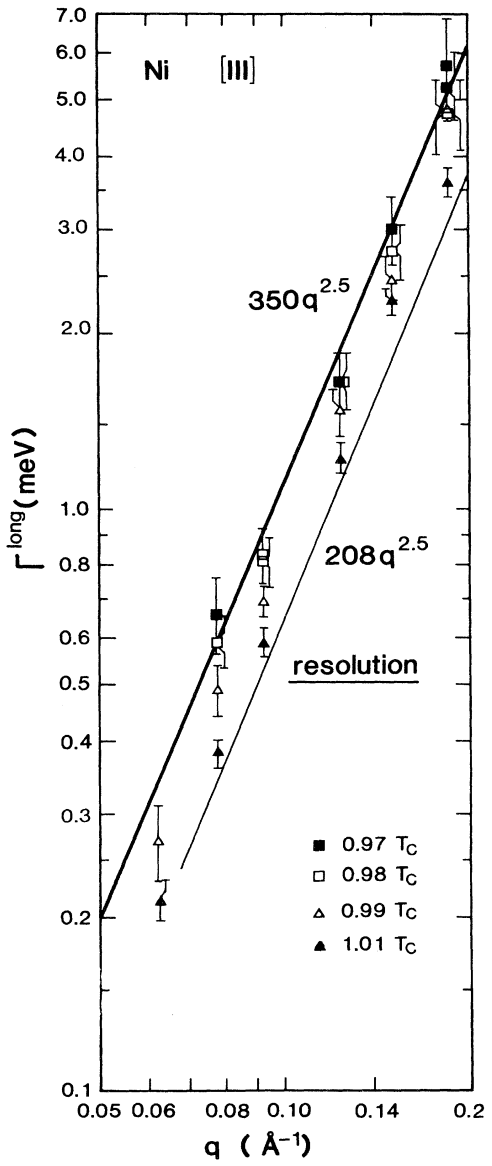

FIG. 8. q dependence of the linewidth of the longitudinal fluctuations. The bold solid line gives Γ at T_C.

Figure 10 demonstrates that the inverse of the energy integrated intensity $I_L(q) = \int d\omega\, S(q,\omega)/k_B T$ is proportional to q^2. In other words, $\chi_L(q)$ can be parametrized by a Lorentzian in q, similar to the paramagnetic fluctuations $\chi_p(q)$, with a correlation length $\xi = 1/\kappa_L$ that increases with increasing T. The transverse intensities are independent of T for $0.97T_c \leq T < 0.99T_C$, as expected from spin-wave theory. Note that the dashed line is displaced by $+4$ in order to enhance the visibility of the data. The inverse correlation length $\kappa_T = 0$ is within the accuracy of the experiment, as expected, because the system is in its long-range ordered ferromagnetic state. The lines through the data points are parametrizations based

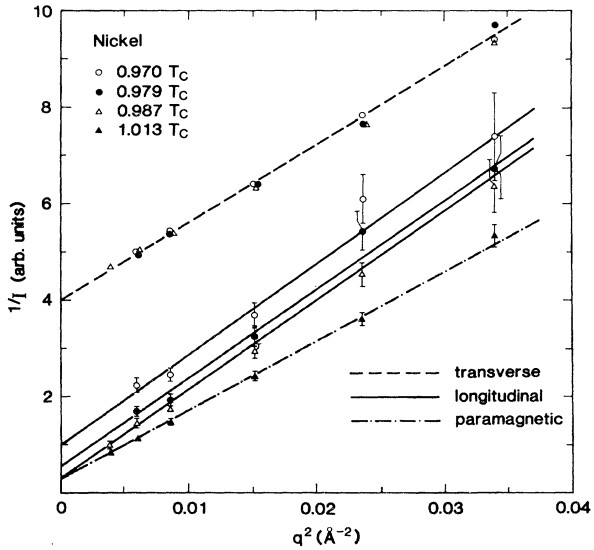

FIG. 10. Inverse integrated neutron intensity vs q^2. The data for the transverse fluctuations (dashed line) are directly proportional to q^2 and is shifted by $I^{-1}=4$ in order to increase the visibility of the data. Paramagnetic scattering data (dashed line) is also included.

on Eq. (4). The fitted static susceptibilities $\chi_i(0)$ and the inverse correlation lengths κ_i obtained in this way are plotted in Figs. 11 and 12 versus T/T_C.

The solid lines are calculations based on the assumption that the critical exponents γ and ν are the same as in the paramagnetic phase [$t=(T-T_C)/T_C$], as implied by scaling theories. The only adjustable parameters were a normalization constant for χ_L and the coefficient for the inverse correlation length κ_0. The critical exponents are from Ref. 8. Within the accuracy of the measurements our data are compatible with critical behavior. Moreover, $\kappa_0=0.81\pm0.04$ Å^{-1} compares well with the value 0.79 ± 0.02 Å^{-1} measured by Anders and Stierstadt by means of small-angle neutron scattering.[33]

Our data indicate that $\kappa_L(-t)\simeq\kappa_p(t)\equiv\kappa(|t|)$, in contrast to the mean-field theory where $\kappa_L=\sqrt{2}\kappa_p$ (Ref. 34), a discrepancy to be expected within the limitations of mean field theory. Passell *et al.* obtained for EuO $\kappa_L/\kappa_p\simeq2.4$ (Ref. 14). The latter discrepancy is also not surprising because (i) the longitudinal fluctuations could not be measured directly in EuO due to the lack of polarized neutrons, and (ii) the dipolar interactions in EuO are strong.[35] In that respect, the data cannot be compared. Clearly, further data are needed to establish the T dependences of χ_L and κ_L more accurately. The influence of magnetic fields has to be considered as well.

Finally, we show the temperature dependence of the spin dynamics in more detail. The spin-wave energy ω_q as measured in the transverse scans is plotted versus q^2 in Fig. 9. The fits (solid lines) confirm the dispersion relation for ferromagnets $\omega_q=Dq^2$. The fitted values for D are consistent with the values quoted by Minkiewicz *et al.*[18] that were measured with unpolarized neutrons. The T dependence of D is compatible with critical behavior, namely, $D\propto(-t)^{\mu}$, with $\mu=\nu-\beta=0.34$.[36] The damping of the spin waves is in accordance with the prediction for the Heisenberg model,[37]

$$\Gamma\propto q^4T^2[A+B\ln(k_BT/Dq^2)+C\ln^2(k_BT/Dq^2)]$$

(not shown). We mention that the combination of the q^4 term with the logarithmic terms produces a q dependence of the spin-wave damping that is numerically very similar to $q^{2.5}$ (see Fig. 8).

The T and q dependence of the energy scales of the magnetic scattering are most easily discussed in terms of dynamical scaling functions. According to dynamical scaling theory, the characteristic energy ω_c is given below and above T_C by[36]

$$\omega_c=Af_i(\kappa_i/q)q^z\ , \tag{6}$$

where f_i is a homogeneous function of κ_i/q, and $z=\frac{1}{2}(d+2-\eta)=2.48\simeq2.5$, for $d=3$. The characteristic energy ω_c is the half-area width defined by[36]

$$\int_{-\infty}^{\infty}F(q,\omega)d\omega=2\int_{-\omega_c}^{\omega_c}F(q,\omega)d\omega\ . \tag{7}$$

For the Lorentzian spectral weight function given by Eq. (5),

$$\omega_c=\sqrt{\omega_q^2+\Gamma^2}\ . \tag{8}$$

In Fig. 13, we plot the scaling functions $f_i(x)\equiv\omega_c/Aq^{2.5}$ $(i=p,L,T)$ using $A=350$ meV Å$^{2.5}$ from Refs. 18 and 23, versus $x=\kappa/q$ for the paramagnetic, longitudinal, and transverse fluctuations. Obviously, the three data sets differ qualitatively from each other as expected. A general trend is that all scaling functions approach each other near $x=0.2$, where $f_i(x)\simeq0.8$. The uncertainty of the longitudinal data is rather large because of the more involved data manipulation, but it is not exceptional when compared with older unpolarized neutron-scattering data in the paramagnetic phase. (Note that the zeros of the ordinates are suppressed.) The top of Fig. 13 also includes data points from previous

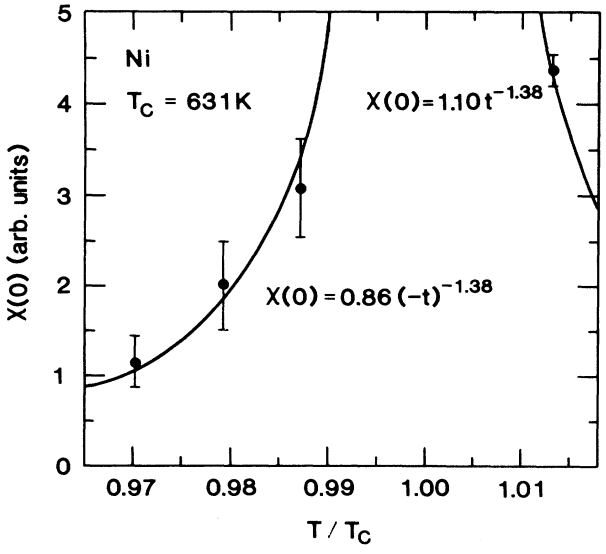

FIG. 11. Temperature dependence of the longitudinal and paramagnetic dc susceptibility. The solid line represents critical behavior.

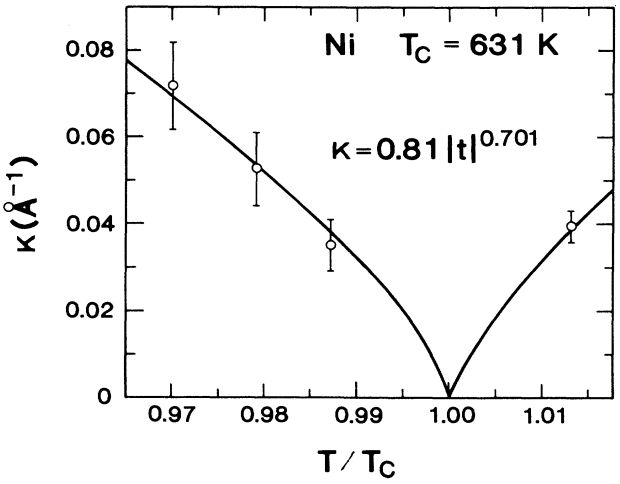

FIG. 12. Temperature dependence of the longitudinal and paramagnetic inverse correlation length. The solid line represents critical behavior.

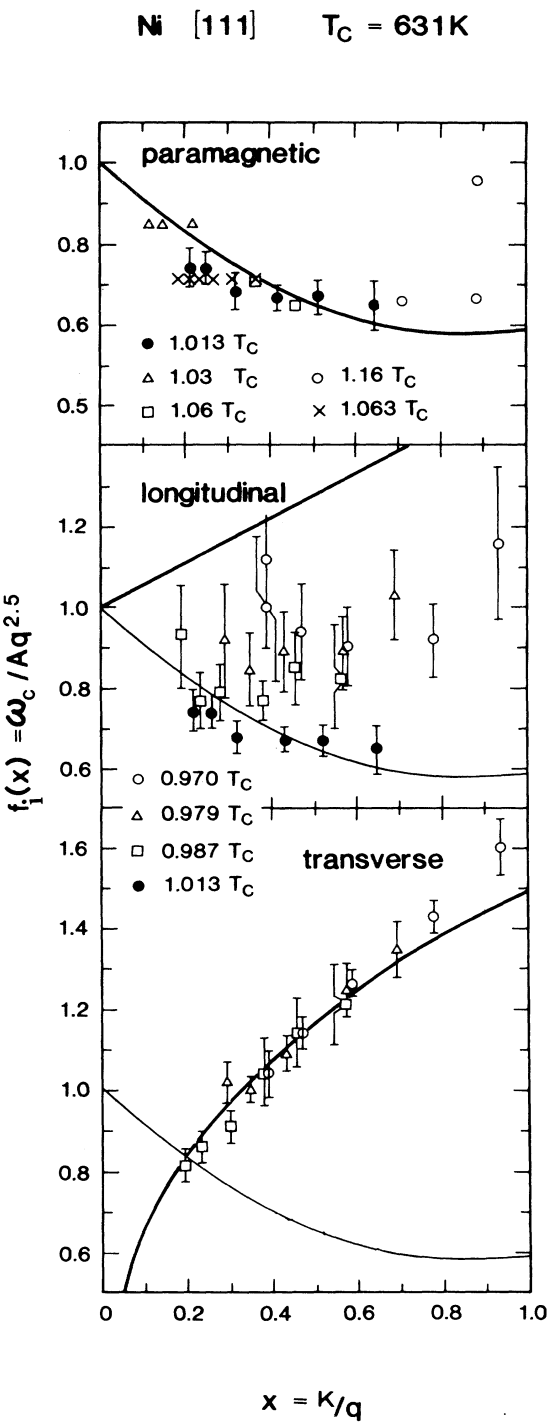

FIG. 13. The paramagnetic, longitudinal, and transverse dynamical scaling functions $f_i(x) \equiv \omega_c / Aq^{2.5}$ ($A = 350$ meV Å$^{2.5}$) vs $x = \kappa/q$. The bold solid lines in the figures represent the dynamical scaling function of Résibois and Piette (Ref. 38) (top), the mode-mode coupling result of Frey and Schwabl (Ref. 1) (center), and the parametrization $f_T(x) = 1.49\sqrt{x}$ (bottom). In the paramagnetic phase (top) the symbols have the following meaning: this study (dots with error bars), Steinsvoll *et al.* (Ref. 23) (circles), Martínez, Böni, and Shirane (Ref. 24) (squares), Shirane, Böni, and Martínez (Ref. 25) (triangles), and Pintschovius (Ref. 26) (crosses).

neutron-scattering studies (symbols without error bars).[23–26] It is gratifying that the data from different works are not only consistent with each other but also in agreement with the Résibois-Piette scaling function[38] within the accuracy of the measurements. We point out that the data for $T = 1.063 T_C$ were measured in the q range $0.306 < q < 0.612$ Å$^{-1} \simeq 0.4 q_{ZB}$, where q_{ZB} corresponds to the zone boundary. At the largest q, the characteristic energy $\omega_c = 73$ meV exceeds even $k_B T_C$. Therefore, the concept of dynamical scaling is useful in Ni over an astonishingly large range of momentum transfers, similar to those in EuO.[39]

IV. DISCUSSION

The paramagnetic scattering data that we observe above T_C agrees well with existing data, indicating that the data collection and analysis were done properly. The inverse correlation length κ is close to the value of Ref. 33. In addition, we have shown that the dynamical scaling function $f_p(x)$ agrees with the theory of Résibois and Piette. Ni is the ideal system for such a comparison because the dipolar interactions are very weak, i.e., $q_D = 0.013$ Å^{-1} is much smaller than the smallest q (0.06 Å^{-1}) we probed in our experiment.

Initially, we were surprised how closely the static behavior of χ_L resembles the critical behavior of $\chi(q)$ above T_C. Qualitatively the Ni data and the EuO data from Ref. 14 resemble the predictions of mean-field theory as mentioned above.[29] Therefore, one may be led to the conclusion that the newer theories, such as renormalization-group and mode-mode coupling, are wrong. In the following we demonstrate that our data are in fact compatible with some predictions of renormalization-group theory and mode-mode coupling theory.

First we discuss the T dependence of $\chi_L(0)$ in the light of an expression given by Wallace[7,8] for finite fields

$$\frac{\chi_L(0) m^{\delta-1}}{\beta} \sim c_1 + c_2 \left[\frac{m^\delta}{h} \right]^{\epsilon/2} + O(1) , \tag{9}$$

which is based on ϵ-expansion techniques in the limit $H \to 0$. Here m is the magnetization in units of the saturation magnetization M_0 at $T = 0$, $c_1 \simeq 0.63$ and $c_2 \simeq 0.20$ are constants,[7] h is the reduced internal magnetic field, and $\epsilon = 4 - d = 1$. Our experiment shows that the influence of the external field H on the magnetic scattering (Fig.5) is small. Indeed, the magnetization changes only by 16% at $0.99 T_C$ due to the external field of 1.1 kOe, if we assume that the demagnetization factor is $N = 0.2$.[40] Therefore, our experiment was conducted in the range $H \to 0$, and m can be replaced in a first approximation by the expression for the spontaneous magnetization $m_0 = B(-t)^\beta$, where $B = 1.52$.[41] In addition, we neglect the field term in Eq. (9). The reason this term is small is not known to us, but a likely explanation is that anisotropy fields, dipolar fields, or fields caused by internal strains and crystal defects quench the divergence. In any case, inserting the expression for m_0 in Eq. (9) yields

$$\chi_L(0) \sim c_1 \beta B^{1-\delta} (-t)^{-\beta(\delta-1)} . \tag{10}$$

The scaling relation $\beta(\delta-1)=\gamma$ shows that the "critical" behavior of $\chi_L(0)$ is actually expected, as long as the internal fields are strong enough to quench the divergence $H^{-1/2}$ at $q=0$, yet weak enough that $m \simeq m_0$. It is interesting to note that bulk measurements by Høg and Johannson in EuO (Ref. 42) and by Kötzler in EuS (Ref. 43) also indicated a similar T dependence of the longitudinal susceptibility $\chi_L(q=0)$. We note that the amplitude ratio χ_p/χ_L in our experiment (single crystal) is 1.3, in contrast to 3.4 for a polycrystalline Ni ring.[41] This apparent discrepancy needs further investigation because the bulk experiment was performed under very different conditions from ours and the influence of the dipolar interactions on the longitudinal fluctuations have yet to be investigated.

In an extension of renormalization-group techniques to finite q, Mazenko[9] obtained for a Heisenberg ferromagnet in three dimensions and zero field

$$\chi_L(q) \simeq \frac{q_D^2}{q^2+\kappa_c^2[14.5/(9+2\kappa_c/q)]} , \tag{11}$$

where we have neglected some unimportant logarithmic terms.[44] The inverse coherence length κ_c is given by um^2. m is the reduced magnetization defined above, and u is the coefficient of the fourth-order term of the order parameter in the expression of the Landau-Ginzburg free energy. If we assume that κ_c can be replaced by our measured values for κ, then Eq. (11) yields Lorentzian behavior ($2\kappa_c/q \ll 9$ for our experiment), in agreement with our data (Fig. 10). Because $um^2 \propto (-t)^{2\beta}$ and $2\beta \simeq \nu$, theory predicts that κ_c should show critical behavior near T_C just as we observe in Fig. 12. For $T \to T_C$, Eq. (11) predicts the well-known result that $\chi_L(q)$ diverges as $1/q^2$, like χ_T and χ_p.

In the opposite limit, $2\kappa_c/q \gg 9$, we obtain

$$\chi_l(q) \simeq \frac{q_D^2}{q^2+7.25q\kappa_c} \propto \frac{1}{\kappa_c q} . \tag{12}$$

This result is in agreement with mode-mode coupling theory in the hydrodynamic limit[11,12] and the prediction of spin-wave theory, i.e., $\chi_L(q=0)=\infty$ for $H=0$.

The above considerations indicate that within the q range of our experiment renormalization-group theory as well as mode-mode coupling theory are compatible with the mean-field-like behavior of $\chi_L(q)$ that we observe in our experiment. In order to measure the $1/\kappa q$ divergence and the field effects on the longitudinal fluctuations, one should extend the measurements to much smaller q.

Finally, we turn to a discussion of the dynamical aspects of the spin fluctuations. Figures 7 and 8 show that the linewidths Γ_i, $i=L,T,p$, are roughly proportional to $q^{2.5}$ as expected from dynamical scaling. Below T_C, Γ_L decreases with increasing T (Fig. 8), as Γ_p. At T_C, the dynamical scaling functions must become identical, in particular $f_L(0)=f_T(0)=f_p(0)$. Our experiment indicates that the longitudinal, as well as the transverse, scaling function becomes smaller than one just below T_C; therefore, f_L and f_T decrease first with increasing x similar to f_p. Although the accuracy of our data is limited, it seems to be incompatible with the predictions of the mode-mode coupling theory by Frey and Schwabl,[1] which predicts that $f_L(x)$ is always greater than one.

The scaling function f_T for the transverse fluctuations (Fig. 13) can be parametrized by $f_T(x)=1.49\sqrt{x}$ ($x=\kappa_L/q$) in the whole range of our measurements, in accordance with the dynamical scaling prediction Eq. (6). For comparison, Passell *et al.* measured $f_T=2.7\sqrt{\kappa_p/q}=1.7\sqrt{x}$ for EuO.[14] The characteristic energy ω_c is mainly determined by the renormalization of the spin waves because they are not heavily damped in the T and q ranges investigated. Therefore, D is almost proportional to $\sqrt{\kappa}$. Mode-mode coupling theory predicts

$$f_T(x)/\sqrt{x}=\pi^{3/2}/5.1326=1.08$$

(Ref. 1), a value that is about 30% smaller than our experimental value 1.49. Nevertheless, the dynamics of the transverse fluctuations below T_C suggest a similar correlation length as the statics of $\chi_L(q)$.

Within the q and T range investigated, we did not find any peaks at finite energy in the longitudinal scattering, even when we tried to force fits to produce spin-wave-like excitations. Therefore the longitudinal fluctuations are diffusive as predicted by the mode-mode coupling theory of Frey and Schwabl[1] and the renormalization-group calculation by Mazenko.[9] However, because our measurements were done for $q > \kappa$, we cannot exclude spin-wave-like excitations in the hydrodynamic region $q \ll \kappa$ as predicted by Villain[11,12] and Vaks, Larkin, and Pikin.[16]

V. SUMMARY

By means of polarized neutron scattering, we have observed unambiguously the longitudinal spin fluctuations in Ni below T_C. Most characteristics of the statics and the dynamics resemble the paramagnetic scattering above T_C. In particular the dc susceptibility χ_L and the correlation length show critical behavior, in agreement with predictions of renormalization-group theory. The correlation lengths below and above T_C are similar. No hint of the expected divergence of $\chi_L(q=0)$ in zero field is visible, which is most likely because of anisotropy fields and sample imperfections. From the dynamics of the magnetic scattering we have extracted the scaling functions for the longitudinal, transverse (spin wave), and paramagnetic scattering. The latter is in good agreement with the Résibois-Piette scaling function for an isotropic ferromagnet.

ACKNOWLEDGMENTS

We thank G. Shirane for the loan of the isotopically enriched ^{60}Ni single crystal and J. Kötzler for the extremely helpful discussions about static susceptibilities and for the estimate in Ref. 40. Research at Brookhaven National Laboratory is supported by the Division of Material Sciences of the Office of Basic Energy Sciences, U.S. Department of Energy under Contract No. DE-AC02-76CH00016.

[1]E. Frey and F. Schwabl, Z. Phys. B **71**, 355 (1988).
[2]E. Frey and F. Schwabl, Phys. Lett. A **123**, 49 (1987); E. Frey, F. Schwabl, and S. Thoma, *ibid.* **129**, 343 (1988); Phys. Rev. B **40**, 7199 (1989).
[3]C. Aberger and R. Folk, Phys. Rev. B **38**, 6693 (1988); **38**, 7207 (1988).
[4]T. Holstein and H. Primakoff, Phys. Rev. **58**, 1098 (1940).
[5]E. Brézin, D. J. Wallace, and K. G. Wilson, Phys. Rev. B **7**, 232 (1973).
[6]E. Brézin and D. J. Wallace, Phys. Rev. B **7**, 1967 (1973).
[7]D. J. Wallace and R. K. P. Zia, Phys. Rev. B **11**, 5340 (1975).
[8]D. J. Wallace, in *Phase Transitions and Critical Phenomena,* edited by C. Domb and M. S. Green (Academic, London, 1976), Vol. 6, p. 293.
[9]G. F. Mazenko, Phys. Rev. B **14**, 3933 (1976).
[10]L. Schäfer and H. Horner, Z. Phys. B **29**, 251 (1978).
[11]J. Villain, Solid State Commun. **8**, 31 (1970).
[12]J. Villain, in *Critical Phenomena in Alloys, Magnets and Superconductors,* edited by R. E. Mills, E. Ascher, and R. I. Jaffee (McGraw-Hill, New York, 1971), p. 423.
[13]J. Kötzler and M. Muschke, Phys. Rev. B **34**, 3543 (1986).
[14]L. Passell, O. W. Dietrich, and J. Als-Nielsen, Phys. Rev. B **14**, 4897 (1976); **14**, 4908 (1976); **14**, 4923 (1976).
[15]P. W. Mitchell, R. A. Cowley, and R. Pynn, J. Phys. C **17**, L875 (1984).
[16]V. G. Vaks, A. I. Larkin, and S. A. Pikin, Zh. Eksp. Teor. Fiz. **53**, 1089 (1967) [Sov. Phys. JETP **26**, 647 (1968)].
[17]M. F. Collins, V. J. Minkiewicz, R. Nathans, L. Passell, and G. Shirane, Phys. Rev. **179**, 417 (1969).
[18]V. J. Minkiewicz, M. F. Collins, R. Nathans, and G. Shirane, Phys. Rev. **182**, 624 (1969).
[19]P. M. Horn, J. M. Hastings, and L. M. Corliss, Phys. Rev. Lett. **40**, 126 (1978).
[20]P. Fulde and A. Luther, Phys. Rev. **170**, 570 (1968).
[21]K. Tajima, P. Böni, G. Shirane, Y. Ishikawa, and M. Koghi, Phys. Rev. B **35**, 274 (1987).
[22]P. Böni and S. M. Shapiro, J. Phys. Condens. Matter **1**, 6123 (1989).
[23]O. Steinsvoll, C. F. Majkrzak, G. Shirane, and J. P. Wicksted, Phys. Rev. Lett. **51**, 300 (1983); Phys. Rev. B **30**, 2377 (1984).
[24]J. L. Martínez, P. Böni, and G. Shirane, Phys. Rev. B **32**, 7037 (1985).
[25]G. Shirane, P. Böni, and J. L. Martínez, Phys. Rev. B **36**, 881 (1987).
[26]L. Pintschovius, Physica B **156**, 709 (1989).
[27]J. A. Hertz, Int. J. Magn. **1**, 253 (1971); **1**, 307 (1971); **1**, 313 (1971).
[28]J. Kötzler, Phys. Rev. B **38**, 12 027 (1988).
[29]W. Marshall and S. W. Lovesey, *Theory of Thermal Neutron Scattering* (Clarendon, Oxford, 1971).
[30]P. Böni and J. L. Martínez (unpublished).
[31]R. A. Cowley, G. Shirane, R. J. Birgeneau, and H. J. Guggenheim, Phys. Rev. B **15**, 4292 (1977).
[32]The effect of higher-order neutrons in the incident neutron beam is an energy-dependent counting time. For instance, at low-incident neutron energies, the counting time is shorter than at higher energies, because the order contamination of the beam is more significant at low energies due to the temperature of the moderator and the structure factor of the Heusler monochromator. During the course of our data analysis, it became apparent that the known monotonic correction factors for pyrolytic graphite and a moderator temperature of 323 K can be used.
[33]R. Anders and K. Stierstadt, Solid State Commun. **39**, 185 (1981).
[34]S. K. Ma, *Modern Theory of Critical Phenomena* (Benjamin, London, 1976).
[35]J. Kötzler, D Görlitz, F. Mezei, and B. Farago, Europhys. Lett. **1**, 675 (1986).
[36]P. I. Halperin and P. C. Hohenberg, Phys. Rev. Lett. **19**, 700 (1967); Phys. Rev. **177**, 952 (1969); Rev. Mod. Phys. **49**, 435 (1977).
[37]See, for example, A. B. Harris, Phys. Rev. **175**, 674 (1968); V. N. Kashcheev and M. A. Krivoglaz, Fiz. Tverd. Tela (Leningrad) **3**, 1541 (1961) [Sov. Phys. Solid State **3**, 1117 (1961)].
[38]P. Résibois and C. Piette, Phys. Rev. Lett. **24**, 514 (1970); C. Joukoff-Piette and P. Résibois, Phys. Lett. **42A**, 531 (1973).
[39]P. Böni and G. Shirane, Phys. Rev. B **33**, 3012 (1986).
[40]Estimate of N by J. Kötzler.
[41]N. Stüsser, M. Th. Rekveldt, and T. Spruijt, Phys. Rev. B **33**, 6423 (1986). For the determination of B the authors have assumed that the paraeffects below T_C are proportional to $(-t)^{-\gamma}$.
[42]J. Høg and T. Johannson, Int. J. Magn. **4**, 11 (1973).
[43]J. Kötzler, J. Magn. Magn. Mater. **54-57**, 649 (1986); see also Ref. 13.
[44]For $x \rightarrow \infty$ the logarithmic terms are less than $\frac{1}{29}$ of the other terms. For $x \rightarrow 0$ these terms go to zero.